On the Prediction of Failure at a Fiber/Matrix Interface in a Composite Subjected to a Transverse Tensile Load

E. S. FOLIAS
University of Utah
Department of Mechanical Engineering
Salt Lake City, UT 84112

(Received January 26, 1990)
(Revised June 25, 1990)

ABSTRACT: This paper deals with the 3-D stress field of a cylindrical fiber which is embedded into a resin matrix. The composite is then subjected to a uniform tensile load σ_o. The strain energy release rate is computed and the criterion is used to predict debonding initiation at the fiber/matrix interface. The analysis shows that this failure is most likely to occur at the free surface, i.e. the region where the fiber intersects a free surface, for example a hole, an edge, or a crack. Moreover, it will occur at approximately (1/10) the load value required for the same failure to commence at the center of the fiber length.

The results are also extended to include a doubly periodic array of fibers which are embedded into a matrix. Based on 3-D considerations, the stiffness matrix is shown to increase as the volume fraction of the fibers increases. Similarly, the stress σ_{rr} in the matrix is shown to decrease as the volume fraction of the fibers increases.

INTRODUCTION

IT IS WELL recognized that fiber composite materials are very attractive for use in aerospace, automotive and other applications. These composites consist of relatively stiff fibers which are embedded into a lower stiffness matrix. Although in most designs the fibers are aligned so that they are parallel to the direction of the external loads, it is almost impossible to avoid induced transverse stresses which may lead to premature failure of the laminate. An excellent example of this is the case of a filament wound pressure vessel in which the presence of a curvature induces bending as well as transverse stresses (Folias, 1965). However, in order to be able to predict their failing characteristics, particularly in the neighborhood of free surfaces such as holes, edges, etc., it is necessary to know the local stress behavior from a 3-D point of view.

An overall summary of some of the results, which are based on 2-D elasticity considerations can be found in the books by Hull (1981) and by Chamis (1975). In their pioneering work, Adams and Doner (1967) used finite differences to solve

0021-9983/91/07 0869-18 $6.00/0

the problem of a doubly periodic array of elastic fibers contained in an elastic matrix and subjected to a transverse load. Their results reveal the dependence of the maximum principal stress versus the constituent stiffness ratio (E_f/E_m) for various fiber volume ratios. A few years later, Yu and Sendeckyj (1974) used a complex variable approach to solve the problem of multiple inclusions embedded into an infinite matrix. Their results were subsequently specialized to cases of two and three inclusions thus providing us with further insight into the strength of the composite. On the other hand, the separation of a smooth circular inclusion from a matrix was investigated by Keer, Dundurs and Kiattikomol (1973). By using finite integral transforms, they were able to reduce the problem to that of a Fredholm integral equation with a weakly singular kernel. Thus, extracting the singular part of the solution, they were able to reduce the remaining problem to a simpler one which lends itself to an effective numerical solution. Their results are very general and are applicable to various combinations of material properties and loads.

In this paper, use of the local, 3-D, stress field will be made in order to examine the dependence of the stress σ_{rr}, in the matrix, on the ratio (G_f/G_m). The strain energy release rate will then be computed in order to predict crack initiation at the fiber/matrix interface. Particular emphasis will be placed in the region where fibers meet a free surface as well as at the center of a fiber's length.

FORMULATION OF THE PROBLEM

Let us consider a cylindrical fiber of homogeneous and isotropic material, e.g., a glass fiber, which is embedded into a matrix of also homogeneous and isotropic material.

Furthermore, we assume the matrix to be a rectangular plate with infinite dimensions $2w$, 2ℓ, and $2h$ as defined by Figure 1. For simplicity, we assume $(w/a) > 8$ and $(\ell/a) > 8$. Such an assumption will guarantee that the boundary planes $x = \pm w$, and $y = \pm \ell$, will not affect the local stress field adjacent to the fiber.[1] Thus mathematically, one may consider the boundaries in the x and y directions to extend to infinity. As to loading, the plate is subjected to a uniform tensile load σ_o in the direction of the y-axis and parallel to the bounding planes (see Figure 1).

In the absence of body forces, the coupled differential equations governing the displacement functions $u_i^{(j)}$ are

$$\frac{1}{1-2\nu_j}\frac{\partial e^{(j)}}{\partial x_i} + \nabla^2 u_i^{(j)} = 0 \qquad i = 1,2,3 \quad j = 1,2 \tag{1}$$

where ∇^2 is the Laplacian operator, ν_j is Poisson's ratio, $u_i^{(1)}$ and $u_i^{(2)}$ represent the displacement functions in media 1 (matrix) and 2 (fiber), respectively, and

$$e^{(j)} = \frac{\partial u_i^{(j)}}{\partial x_i} \qquad i = 1,2,3 \quad j = 1,2 \tag{2}$$

[1]This can be seen from the results which were recently reported by Penado and Folias (1989).

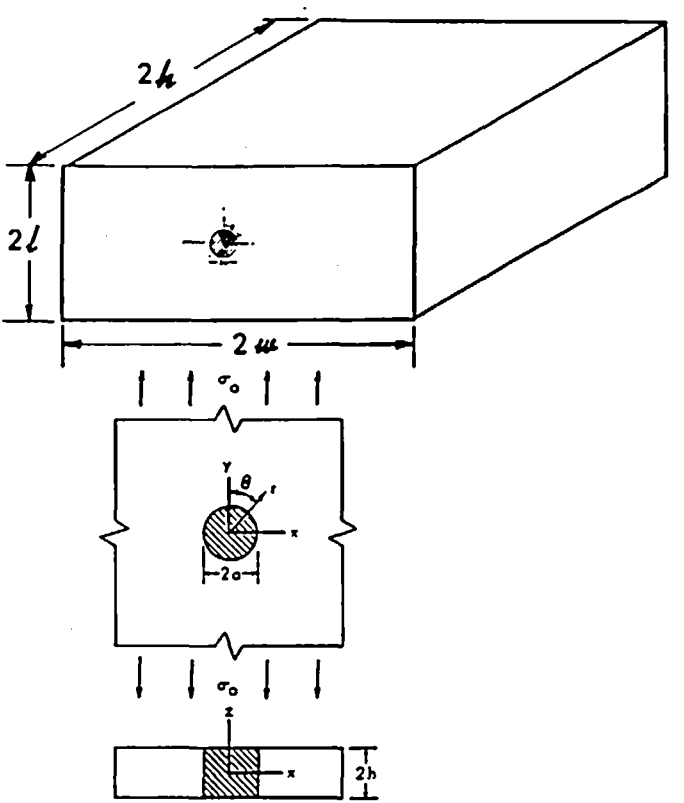

Figure 1. *Geometrical and loading configurations.*

The stress-displacement relations are given by Hooke's law as

$$\sigma_{ij}^{(j)} = \lambda_j e_{kk}^{(j)} \delta_{ij} + 2G^{(j)} e_{ij}^{(j)} \tag{3}$$

where λ_j and G_j are the Lamé constants describing media 1 and 2.

THE SOLUTION FOR ONE FIBER

A. Region Where Fiber Intersects the Free Edge

This problem was recently investigated by the author (Folias, 1989) who was able to recover, explicitly, the three-dimensional stress field adjacent to the surface of the fiber.[2] Without going into the mathematical details, the displacement

[2]A similar analysis for a transversely isotropic fiber meeting a free surface has recently been completed and the results will be reported soon.

and stress fields for the matrix are given in terms of the local coordinate system (see Figure 2) by:

1. DISPLACEMENT FIELD

$$u^{(1)} = A_n\varrho^{\alpha-1}\sin\theta\{B[2(1-\nu_1)\cos(\alpha-1)\phi - (\alpha-1)\sin\phi\sin(\alpha-2)\phi] - (\alpha+1)[(1-2\nu_1)\sin(\alpha-1)\phi + (\alpha-1)\sin\phi\cos(\alpha-2)\phi]\}\cos(2n\theta) \quad (4)$$

$$v^{(1)} = A_n\varrho^{\alpha-1}\cos\theta\{B[2(1-\nu_1)\cos(\alpha-1)\phi - (\alpha-1)\sin\phi\sin(\alpha-2)\phi] - (\alpha+1)[(1-2\nu_1)\sin(\alpha-1)\phi + (\alpha-1)\sin\phi\cos(\alpha-2)\phi]\}\cos(2n\theta) \quad (5)$$

$$w^{(1)} = A_n\varrho^{\alpha-1}\{B[-(1-2\nu_1)\sin(\alpha-1)\phi + (\alpha-1)\sin\phi\cos(\alpha-2)\phi] - (\alpha+1)[2(1-\nu_1)\cos(\alpha-1)\phi + (\alpha-1)\sin\phi\sin(\alpha+2)\phi]\}\cos(2n\theta) \quad (6)$$

2. STRESS FIELD

$$\sigma_{rr}^{(1)} = 2G^{(1)}(\alpha-1)A_n\varrho^{\alpha-2}\{B[2\cos(\alpha-2)\phi - (\alpha-2)\sin\phi\sin(\alpha-3)\phi] - (\alpha+1)[\sin(\alpha-2)\phi + (\alpha-2)\sin\phi\cos(\alpha-3)\phi]\}\cos(2n\theta) \quad (7)$$

$$\sigma_{\theta\theta}^{(1)} = 4\nu_1G^{(1)}(\alpha-1)A_n\varrho^{\alpha-2}\{B\cos(\alpha-2)\phi - (\alpha+1)\sin(\alpha-2)\phi\}\cos(2n\theta) \quad (8)$$

$$\sigma_{zz}^{(1)} = 2G^{(1)}(\alpha-1)A_n\varrho^{\alpha-2}\{B(\alpha-2)\sin\phi\sin(\alpha-3)\phi + (\alpha+1)[(\alpha-2)\sin\phi\cos(\alpha-3)\phi - \sin(\alpha-2)\phi]\}\cos(2n\theta) \quad (9)$$

$$\tau_{rz}^{(1)} = 2G^{(1)}(\alpha-1)A_n\varrho^{\alpha-2}\{B[\sin(\alpha-2)\phi + (\alpha-2)\sin\phi\cos(\alpha-3)\phi] - (\alpha+1)(\alpha-2)\sin\phi\sin(\alpha-3)\phi\}\cos(2n\theta) \quad (10)$$

$$\tau_{r\theta}^{(1)} = \tau_{\theta z}^{(1)} = 0 \quad (11)\text{-}(12)$$

where $n = 0,1,2,\ldots$ and B is a function of the material constants and A_n is a constant to be determined from the boundary conditions far away from the fiber.[3]

[3]For one fiber $n = 0,1.$, while for a periodic extension $n = 0,1,2,\ldots$

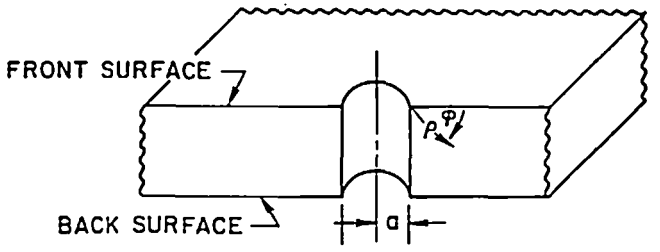

Figure 2. *Definition of local coordinates.*

In general, the characteristic value of α depends on the material constants of the fiber as well as of the matrix. A typical example is given in Figure 3.

Upon examination of the stress field, the following remarks are worthy of note. First, the stress field in the neighborhood where the fiber meets the free surface is singular. Moreover, in the limiting case of a perfectly rigid inclusion this singularity strength reaches the value of 0.2888. Second, boundary conditions $\sigma_{zz}^{(1)}$, $\tau_{xz}^{(1)}$ and $\tau_{yz}^{(1)}$ are satisfied as a consequence of the odd functional behavior in ϕ,

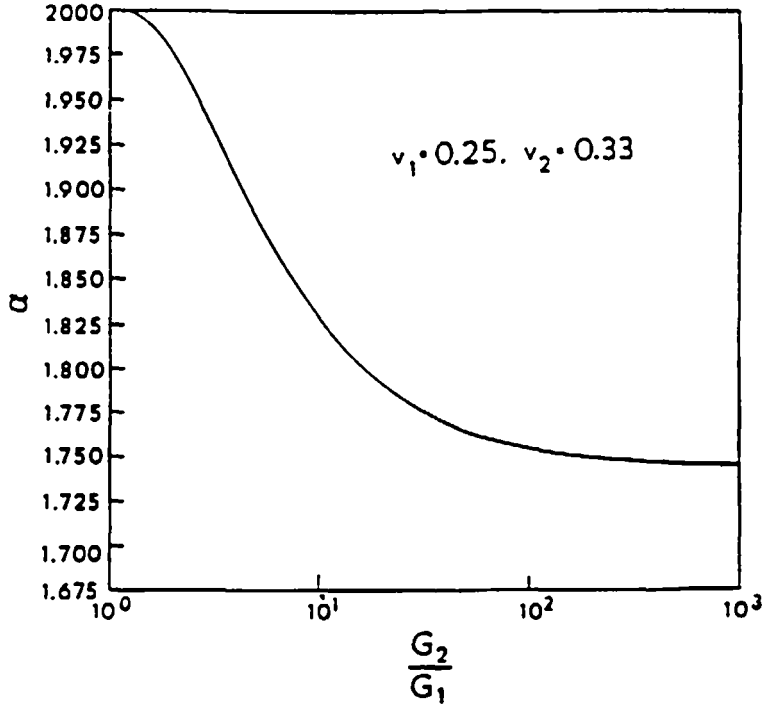

Figure 3. *Singularity strength for isotropic fiber and isotropic matrix versus G_2/G_1.*

which points to the presence of a boundary layer solution as one approaches the free surface. Third, on the free surface the radial stress is $(1/\nu_1)$ times the circumferential stress. This suggests, therefore, that if a crack was to initiate, it would propagate along (or very, very close to) the fiber/matrix interface. Clearly, the occurrence of either adhesive or cohesive failure will depend on the relative strengths of the interface, of the fiber, and of the matrix. All things being equal, the analysis shows the stresses to be highest at the interface, thus pointing to an adhesive type of failure.

B. Interior Region

The 3-D stress field for this region has also been recovered by Penado and Folias (1989) and the results for various (a/h) and (G_2/G_1) ratios may be found in the literature. The results have subsequently been extended (Folias and Liu, 1990) to also include a layer of modified matrix around the fiber. Thus for $\nu_1 = 0.34$, $\nu_2 = 0.22$ and $(G_2/G_1) = 16.67$ the stresses $\sigma_{rr}^{(1)}$ and $\sigma_{\theta\theta}^{(1)}$ at $r = a$ and for all $|z| \leq h$ are given in Figures 4 and 5, respectively. Finally, Figure 6 (for $\lambda = 0$) shows the variation of the stress $\sigma_{rr}^{(1)}$ as a function of the ratio (G_2/G_1).

INTERFACE FAILURE CLOSE TO THE FREE SURFACE

A closer inspection of the local stress field shows that a crack is most likely to initiate at the location $\theta = 0$ and subsequently propagate along the fiber/matrix

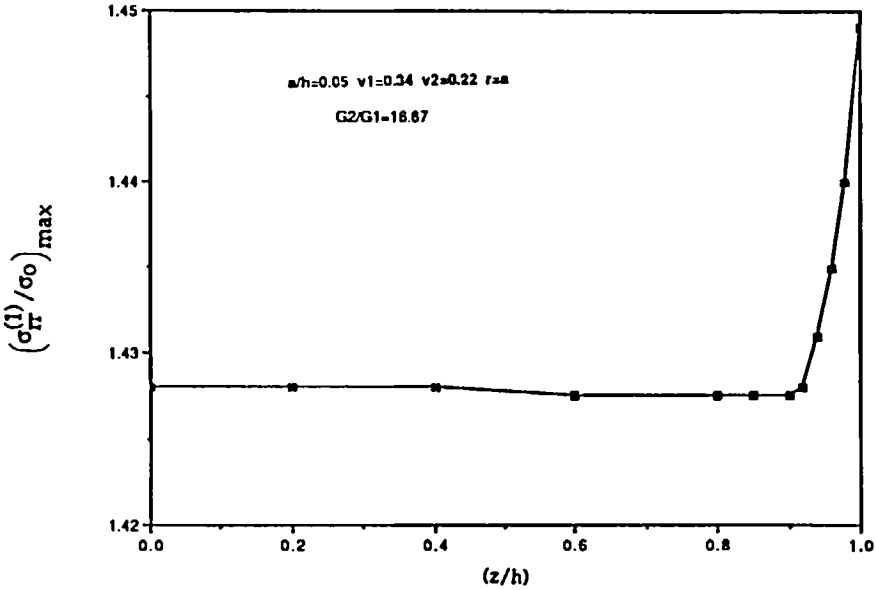

Figure 4. Stress $\sigma_{rr}^{(1)}$ at $r = a$, $\theta = 0$ and for $\nu_1 = 0.34$, $\nu_2 = 0.22$ and $(G_2/G_1) = 16.67$, across the thickness.

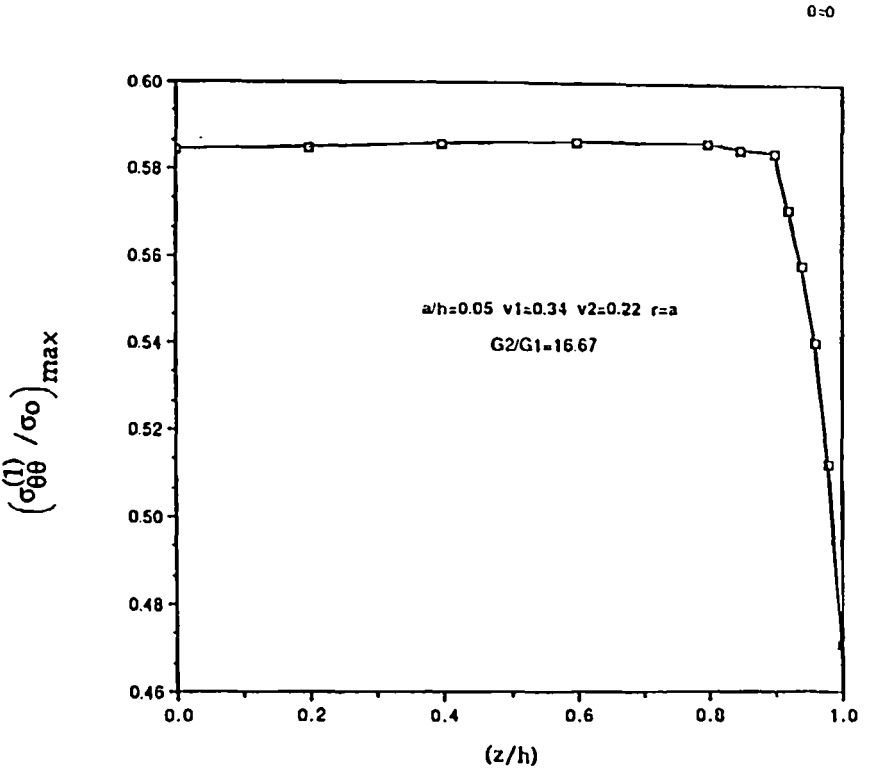

Figure 5. *Stress $\sigma_{\theta\theta}^{(1)}$ at $r = a$, $\theta = 0$ and for $\nu_1 = 0.34$, $\nu_2 = 0.22$ and $(G_2/G_1) = 16.67$, across the thickness.*

interface until it reaches a nominal value of the arc length beyond which it will advance into the matrix. Moreover, once the crack begins to propagate, it will simultaneously propagate along the interface and parallel to the axis of the fiber (mode III). Thus, crack propagation will be governed initially by a mode I failure and subsequently by a combination of mode I and mode III failure. It is now possible for us to examine the first stage of the failing process and to obtain an estimate of the debonded arc length as well as an estimate of the critical transverse stress for crack initiation.

As a practical matter, we will consider the special case of a glass fiber embedded into an epoxy matrix with the following properties

$$\begin{aligned} G_1 &= 2.10 \text{ GPa} & \nu_1 &= 0.34 \\ G_2 &= 35.00 \text{ GPa} & \nu_2 &= 0.22 \end{aligned} \tag{13}$$

Without going into the numerical details, the constants α, A and B for this example are found to be[4]:

$$\alpha = 1.7511 \qquad G^{(1)}Aa^{\alpha-2} \approx 0.6349\sigma_o \qquad B \approx 2.1302 \tag{14}$$

where σ_o now has the units of GPa. Thus, from Equations (7)–(12) one has

(1) At $\phi = 0$ and $\theta = 0$:

$$\sigma_{rr}^{(1)} \approx 4.0633\sigma_o \left(\frac{r-a}{a}\right)^{-0.2489} \tag{15}$$

$$\sigma_{\theta\theta}^{(1)} = \nu_1 \sigma_{rr}^{(1)} \tag{16}$$

(2) At $\phi = \pi/2$ and $\theta = 0$:

$$\sigma_{rr}^{(1)} \approx 1.9163\sigma_o \left(\frac{h-z}{h}\right)^{-0.2489} \tag{17}$$

$$\sigma_{\theta\theta}^{(1)} \approx 0.4844\sigma_{rr}^{(1)} \tag{18}$$

$$\tau_{rz}^{(1)} \approx -0.2930\sigma_{rr}^{(1)} \tag{19}$$

It is clear now from Equations (15) and (16) that crack failure is most likely to initiate and subsequently propagate along the fiber/matrix interface rather than perpendicular to it. Similarly, Equations (17) and (19) suggest that failure in the direction parallel to the axis of the fiber is dominated first by a mode I and second by a mode III type of failure. It may also be noted that $\sigma_{rr}^{(1)}$ attains a maximum at $\theta = 0$ and decreases as one travels along the surface of the fiber.

Finally, based on 3-D considerations, the stress field away from the edges, $z = \pm h$, and in the interior of the plate was shown to be non-singular (Penado and Folias, 1989; Folias and Liu, 1990) with[5]

$$\sigma_{\theta\theta}^{(1)} = 0.4090 \qquad \sigma_{rr}^{(1)} = 0.4090(1.4281\sigma_o) = 0.5841\sigma_o$$

$$\text{at } \theta = 0 \tag{20a}$$

at $r = a$ and $z = 0$. Comparing this value with that of the corresponding plane strain solution

$$\sigma_{\theta\theta}^{(1)} = \frac{\nu_1}{1-\nu_1} \qquad \sigma_{rr}^{(1)} = 0.5152\sigma_o \qquad \text{at } \theta = 0 \tag{20b}$$

[4]The constant A has been determined by comparing the displacement $w^{(1)}$, as well as the stress $\sigma_{rr}^{(1)}$ at $\theta = 0$, at $z = h$ and for $(a/h) = 0.5$ with the work of Penado and Folias (1989). $A = \Sigma_n A_n$.

[5]These results are valid for a ratio of $(a/h) = 0.05$ and subject to the assumption that $(w/a) > 8$ and $(\ell/a) > 8$ in which case the end boundaries in x and y have insignificant effects on the local to the fiber stress field.

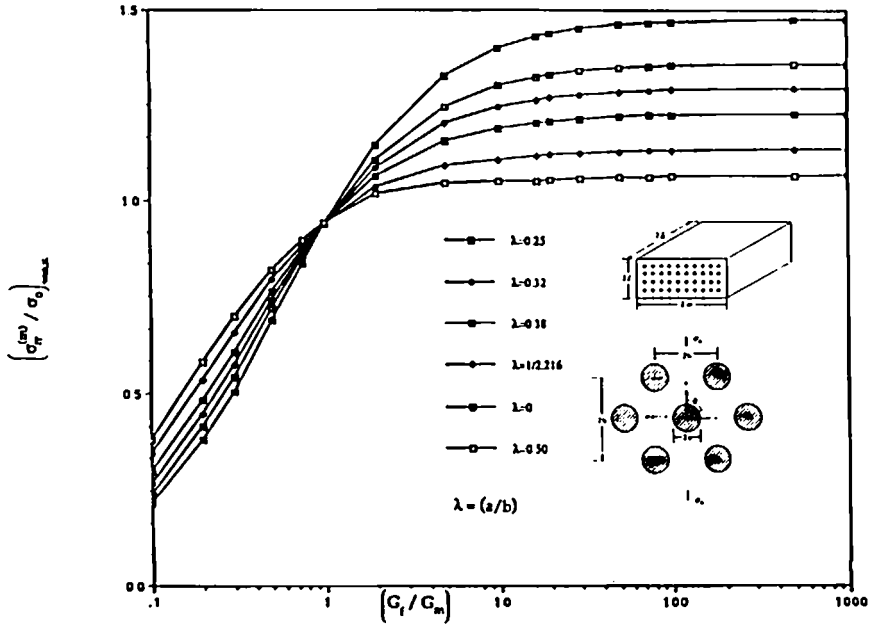

Figure 6. *Stress $\sigma_{rr}^{(1)}$ at $r = a$, $\theta = 0$ and for $\nu_1 = 0.34$, $\nu_2 = 0.22$, versus the ratio (G_2/G_1).*

one notices that it is approximately 13% higher in value due to the presence of the stresses in the third dimension.

It is now possible for us to obtain an approximate criterion for debonding along the fiber/matrix interface based on Griffith's theory of fracture. Thus, following the work of Toya (1974), if one assumes the presence of an interface crack of length $2a\beta$ and if furthermore takes into account the local 3-D stress field, then Toya's result may be written as

$$(1/16)(1.1337\sigma_o)^2 ka\tilde{A}_1(1 + 4\epsilon^2)\pi N_o \bar{N}_o \sin\beta \exp[2\epsilon(\pi - \beta)] = 2\gamma_{12} \tag{21}$$

where

$$k = \frac{1 + k_2}{1 + k_2 + (1 + k_1)(G_2/G_1)} \tag{22}$$

$$k_i = \begin{cases} 3 - 4\nu_i & \text{for plane strain} \\ \dfrac{3 - \nu_i}{1 + \nu_i} & \text{for plane stress} \end{cases} \tag{23}$$

$$\tilde{A}_1 = \frac{k}{4G_1}\{1 + k_1 + (1 + k_2)(G_1/G_2)\} \tag{24}$$

$$\epsilon = -\frac{1}{2\pi}\ln\left[\frac{1 + k_2(G_1/G_2)}{k_1 + (G_1/G_2)}\right] \tag{25}$$

$$N_o = G_o - \frac{1}{k} - \frac{2(1 - k)}{k}\frac{1 + k_2(G_1/G_2)}{k_1 + (G_1/G_2)}\exp[\beta(2\epsilon - i)] \tag{26}$$

$$G_o = \frac{1 - (\cos\beta + 2\epsilon\sin\beta)\exp[2\epsilon(\pi - \beta)] + (1 - k)(1 + 4\epsilon^2)\sin^2\beta}{2 - k - k(\cos\beta + 2\epsilon\sin\beta)\exp[2\epsilon(\pi - \beta)]} \tag{27}$$

where $\bar{N}_o$ is the complex conjugate of N_o, γ_{12} is the specific surface energy of the interface and β the angle of debonded interface (see Figure 7). While it is true that this type of approach does not provide results for the exact initiation of an in-

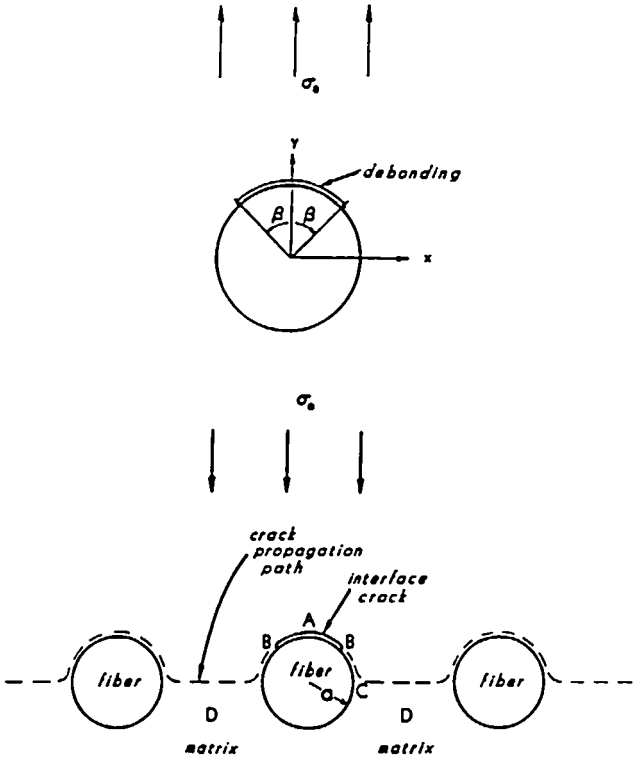

Figure 7. *Fiber/matrix interface crack under transverse loading.*

terface crack problem, i.e., from a condition of perfectly bonded interface to that of a partially debonded interface, it does, however, provide a very good first approximation to this complex phenomenon. The author is well aware of that and is presently continuing his work along such lines and with some promise.

Upon rearranging, Equation (21) can be written in the form[6]

$$\frac{2\gamma_{12}}{\sigma_o^2 a} = (1.2853)F(\nu_i, G_i; \beta) \tag{28}$$

where F is a function of the material constants and the angle β of the debonded interface. A plot of this equation for conditions of plane stress, as well as of plane strain, is given in Figure 8. In both cases the maximum occurs at $\beta = 60°$. Beyond this angle, the crack will gradually curve away from the interface and into the matrix.

In order for us to obtain an estimate for the critical stress for crack initiation we let $\beta \to 0^+$, i.e., very small but not zero. Thus, for our example

$$(\sigma_o)_{cr}\sqrt{2a\beta} \approx 1.8186\sqrt{\gamma_{12}G_1} \quad \text{at } z = 0 \tag{29a}$$

On the other hand, in the neighborhood of the free surface, the applied stress is much higher because of the singularity presence. In order to overcome this difficulty, one may average the local stress over a distance equal to 10% of that of the radius, i.e.

$$(\sigma_o)_{\text{eff}} = \frac{1}{(0.1a)} \int_0^{0.1a} (4.0633\sigma_o)\left(\frac{\xi}{a}\right)^{-0.2489} d\xi \approx 9.5958\sigma_o \tag{30}$$

Thus[7]

$$(9.5958\sigma_o)_{cr}\sqrt{2a\beta} \approx 1.8146\sqrt{\gamma_{12}G_1} \quad \text{at } z \approx \pm h \tag{29b}$$

Combining next Equations (29a) and (29b) one finds

$$\frac{(\sigma_o)_{cr}\,|\,\text{at } z = h}{(\sigma_o)_{cr}\,|\,\text{at } z = 0} \approx 0.10 \tag{31}$$

i.e., the critical loading stress which may cause failure close to a free surface is approximately (1/10) of the critical stress required to cause the same failure at the

[6]It should be noted that at the crack ends the stress field oscillates and that some overlap of the crack faces takes place. This matter is well recognized and has been documented by Williams (1952), Rice et al. (1965) and England (1965). The region where this occurs, however, is so small (less than $a \times 10^{-3}$) that Equation (28) provides a good approximation.

[7]The reader may notice that the right-hand side of Equation (29b) differs from (29a) because it is based on plane stress.

center of the fiber's length. Thus, all things being equal, a crack will initiate at the free surface and will propagate along the periphery of the fiber/matrix interface as well as parallel to the axis of the fiber.

Focusing next our attention on the advancement of the crack along the periphery of the fiber we conclude that the crack will advance itself to a critical angle of $\beta \approx 60°$. Once the crack has reached $\theta = 60°$, the local geometry is similar to that of a hole. This problem has also been investigated for the 3-D stress field close to a free surface (Folias, 1987), as well as in the interior of the plate (Folias and Wang, 1986). Without going into the details, at $z = h$, it was found that

$$\frac{\sigma_{\theta\theta}^{(1)}}{\sigma_{rr}^{(1)}} = -(1 + \nu_1) = -1.34 \tag{32}$$

suggesting, therefore, that the failure now is governed by the stress $\sigma_{\theta\theta}^{(1)}$ which attains its maximum value at $\theta = \pi/2$. Thus, the crack will begin to curve into the matrix until its direction becomes perpendicular to that of the applied load.

PERIODIC ARRAY OF FIBERS

The previous results were based on the presence of one fiber only. It is now desirable to extend these results to also include a doubly periodic array of fibers which are embedded into a matrix. For this reason, we assume a periodic ar-

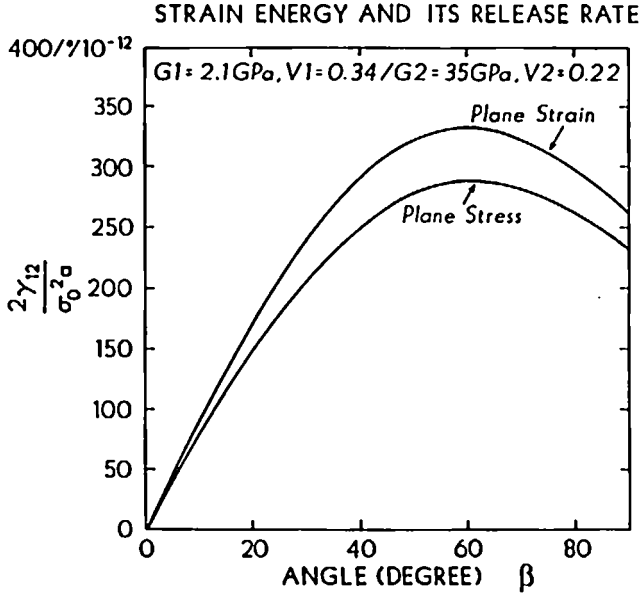

Figure 8. Strain energy release rate for plane stress and plane strain conditions for ν_1 = 0.34, ν_2 = 0.22 and (G_2/G_1) = 16.67.

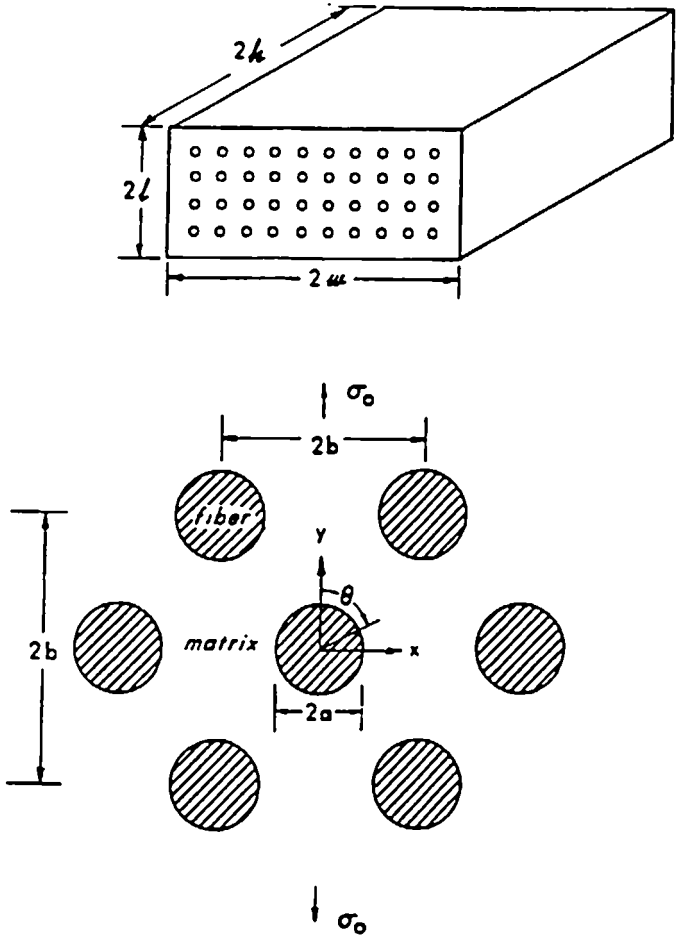

Figure 9. *Periodic array of fibers of length 2h, embedded into a matrix.*

rangement of the type shown in Figure 9. Following the same method of solution as that of Penado and Folias (1989), one finds[8] at $z = 0$ the stresses $\sigma_{rr}^{(1)}$ and $\sigma_{\theta\theta}^{(1)}$, for $\nu_1 = 0.34$, $\nu_2 = 0.22$ and various (G_2/G_1) ratios, shown in Figures 6 and 10. Two observations are worthy of note. First, beyond a certain ratio of (G_2/G_1) the stress $\sigma_{rr}^{(1)}$ reaches an asymptotic value. Such a trend was also found by Adams

[8]The results are valid for all fibers which are at least four diameters away from the bounding planes $x = \pm w$ and $y = \pm \ell$. The solution *and the details* are similar to those discussed by Penado and Folias (1989) except that one now has $\cos(2n\theta)$, $n = 0,1,2,\ldots$, where the remaining unknown coefficients are determined from the boundary conditions of the geometrical cell configuration. The present results are based on $n = 0,\ldots,N = 20$ terms which provide accurate results in the region $|z/h| < 0.9$. However, many more terms are needed in order to obtain accurate results particularly in the neighborhood of $z = \pm h$. We are presently working on this and the results for this problem, as well as for the problem of stresses due to temperature mismatch, will be reported in the near future.

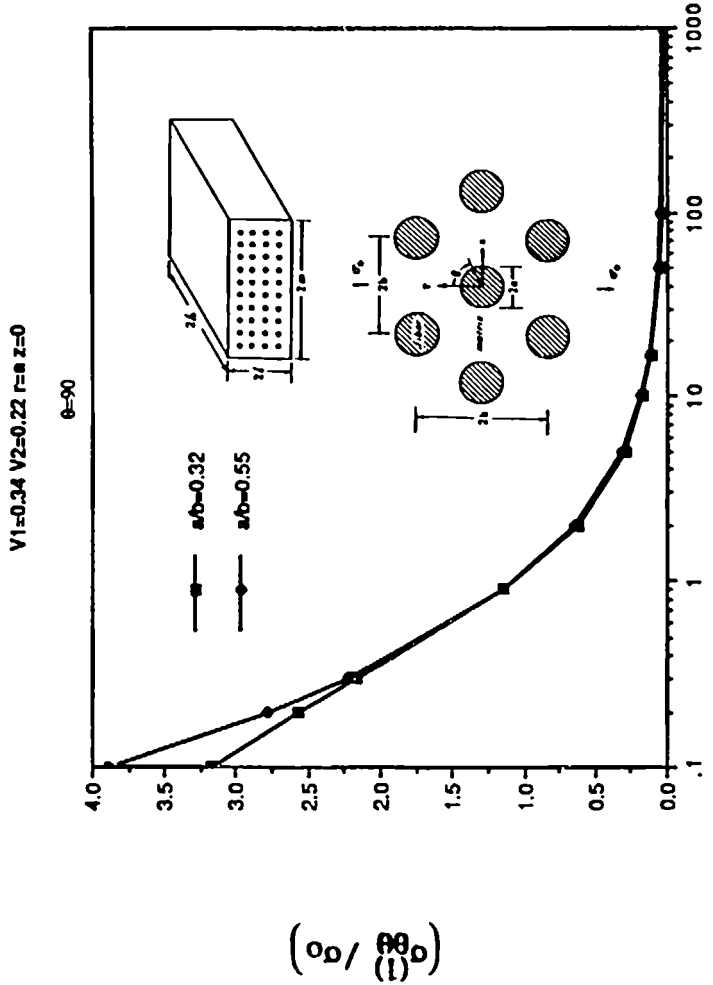

Figure 10. Stress $\sigma_{\theta}^{(1)}$ at $r = a$, $\theta = 0$ and for $\nu_1 = 0.34$, $\nu_2 = 0.22$, versus the ratio (G_2/G_1).

(1967) based on 2-D considerations. Second, as the volume of fibers increases the stress $\sigma_{rr}^{(1)}$ decreases by as much as 40% (see Figure 11).

Returning next to the strain energy release rate, Equation (21) is still a good approximation provided that σ_o is replaced by the following effective load stress

$$(\sigma_o)_{\text{effective periodic}} \approx \left\{ \frac{\sigma_{rr}^{(1)}|_{\lambda}}{\sigma_{rr}^{(1)}|_{\lambda=0}} \right\} \sigma_o \equiv \{F(V_f)\}^{-1}\sigma_o \quad \text{for } z = 0 \tag{33}$$

Thus Equation (29a) now becomes

$$(\sigma_o)_{cr} \approx 1.8186 F(V_f) \sqrt{\frac{\gamma_{12} G_m}{2a_f \beta}} \tag{34}$$

which is valid for small values of β.

Unfortunately, in order to obtain a similar expression for $z = h$, one needs to establish whether the order of the singularity strength increases as adjacent fibers approach the fiber in question. In view of some previous work the author conjectures that this may very well be the case. Thus, the following fundamental questions come to mind. How close must adjacent fibers be before the order of the singularity strength is affected? Does a certain separation distance or a certain periodic array of fibers exist which leads to an optimal state of stress? Based on 3-D considerations, Penado and Folias (1989) have shown that when fibers are placed four fiber diameters apart, center to center, practically all fiber interactions have subsided, including those at the free surface $z = h$. The author suspects, however, that when fibers are placed two diameters apart, center to center, the singularity strength may be affected. Naturally, this is a conjecture that needs to be investigated.

As a practical matter, if one uses the approximation given by Equation (30), the critical stress to failure at the fiber edge in a glass fiber/epoxy matrix composite with the properties

$$\begin{aligned} G_m &= 2.10 \text{ GPa} \quad & \nu_m &= 0.34 \quad & a_f &= 10^{-3} \text{ cm} \quad & \beta &= 60^\circ \\ G_f &= 35.00 \text{ GPa} \quad & \nu_f &= 0.22 \quad & 2\gamma_{12} &= 70 \text{ J/m}^2 \quad & V_f &= 0.70 \end{aligned} \tag{35}$$

becomes

$$\begin{aligned} (\sigma_o)_{cr} &= 20.582\, F(V_f) \text{ MPa} \\ &= 2.985\, F(V_f) \text{ ksi} \quad \text{at the fiber edge} \end{aligned} \tag{36}$$

a plot of which is given in Figure 12. Edge delamination may now be modeled as the progressive failure of a row of fibers.

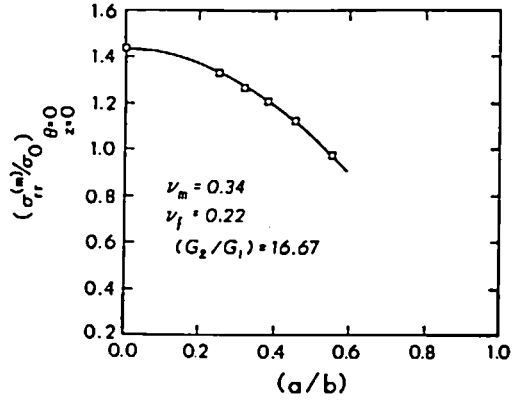

Figure 11. Stress $\sigma_{\theta\theta}^{(1)}$ at r = a, versus V_f, for $(G_2/G_1) = 16.67$ $\nu_1 = 0.34$, $\nu_2 = 0.22$.

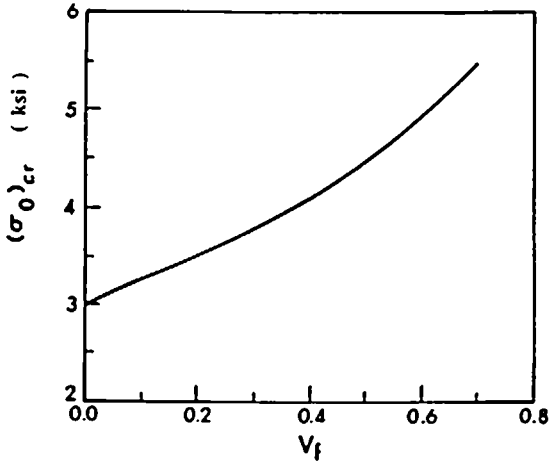

Figure 12. Critical stress to failure versus V_f for $(G_2/G_1) = 16.67$, $\nu_1 = 0.34$ and $\nu_2 = 0.22$.

CONCLUSIONS

Based on a 3-D analytical solution, we have shown that fiber/matrix debonding is most likely to occur close to a free surface. Thus, regions where fibers intersect free surfaces, e.g., holes, cut outs, edges, cracks, etc. are potential trouble spots. Moreover, the strain energy release rate [Equation (28)] may be used to predict crack initiation in the center of the fiber length [Equation (29a)], as well as at the free surface [Equation (29b)]. Moreover, fiber/matrix debonding at a free surface will occur at approximately (1/10) the load value required for the same type of failure to occur at the center of the fiber length. Such information on crack initiation is particularly important for the proper understanding of damage evolution.

Alternatively, the strain energy release rate for a periodic array of fibers of the type shown in Figure 9 may, at $z = 0$, be approximated by Equation (28) in conjunction with Equation (33). A similar expression applicable to the neighborhood of the free surface requires that one must first establish whether the strength of the singularity is indeed affected as the fiber volume increases. For $\bar{V}_f \leq 0.05$, however, it has been shown[9] that no such interaction effects are present.

As a final remark, we note that if the bond at the interface does not fail the analysis shows that there exists a stress magnification factor in the resin which attains a maximum between the fibers. This maximum stress magnification occurs along the line $\theta = 0°$ and at a distance $r = 1.2a$ from the center of the fiber.[10]

ACKNOWLEDGEMENT

This work was supported in part by the Air Force Office of Scientific Research Grant No. AFOSR-87-0204. The author wishes to thank Lt. Col. G. Haritos for this support and for various discussions.

REFERENCES

Adams, D. F. and D. R. Doner. 1967. "Transverse Normal Loading of a Unidirectional Composite," *J. of Composite Materials*, 1:152-164.

Chamis, C. C., ed. 1975. *Composite Materials, Vol. 1-8*. Academic Press.

England, A. H. 1965. "A Crack between Dissimilar Media," *Journal of Applied Mechanics*, pp. 400-402.

Folias, E. S. 1989. "The 3-D Stress Singularities at the Intersection of a Cylindrical Inclusion and a Free Surface," *International Journal of Fracture*, 39:25-34.

Folias, E. S. 1987. "The 3-D Stress Field at the Intersection of a Hole and a Free Surface," *International Journal of Fracture*, 35(3):187-194.

Folias, E. S. 1965. "An Axial Crack in a Pressurized Cylindrical Shell," *International Journal of Fracture*, 1:20-46.

Folias, E. S. and J. Liu. 1990. "The 3-D Stress Field of a Cylindrical Fiber Embedded into a Matrix with a Layer of Modified Matrix around the Fiber" (under review).

Folias, E. S. and J. J. Wang. 1990. "On the Three-Dimensional Stress Field around a Circular Hole in a Plate of an Arbitrary Thickness," *J. of Computational Mechanics*, 6(6):379-391.

[9]See Panado and Folias (1989).

[10]This condition is valid for all $0 \leq z < h$.

Hull, D. 1981. *An Introduction to Composite Materials*. Cambridge University Press.

Keer, L. M., J. Dundurs and K. Kiattikomol. 1973. "Separation of a Smooth Circular Inclusion from a Matrix," *Int. Journal of Engineering Science*, 11:1221-1233.

Penado, F. E. and E. S. Folias. 1989. "The Three-Dimensional Stress Field around a Cylindrical Inclusion in a Plate of Arbitrary Thickness," *International Journal of Fracture*, 39:129-146.

Rice, J. R. and G. C. Sih. 1965. *Journal of Applied Mechanics, Transaction ASME, Series E 32*, p. 418.

Toya, M. 1974. "A Crack along the Interface of a Circular Inclusion Embedded in an Infinite Solid," *Journal of Mechanics and Physics of Solids*, 22:325-348.

Williams, M. L. 1952. *Journal of Applied Mechanics, Transactions ASME*, 19:526.

Yu, I. W. and G. P. Sendeckyj. 1974. "Multiple Circular Inclusion Problems in Plane Elastostatics," pp. 215-220.